Available online at www.sciencedirect.com
SCIENCE DIRECT®
Journal of Chromatography A, 1011 (2003) 11–22
JOURNAL OF CHROMATOGRAPHY A
www.elsevier.com/locate/chroma

Analysis of active sites and heterogeneity in commercial reversed-phase octadecylsilanated silica with numerically calculated sorption distributions

Brett J. Stanley*, Jolie Krance[1]
Department of Chemistry, California State University, 5500 University Parkway, San Bernardino, CA 92407-2397, USA

Received 6 March 2003; received in revised form 12 June 2003; accepted 26 June 2003

Abstract

Sorption isotherms spanning six orders of magnitude of pyridine concentration in a 60:40 methanol:water mobile phase adjusted to pH 5 were obtained with the frontal analysis method on three ODS stationary phases: Zorbax Pro-10/150, Vydac 218TPB10, and YMC 120AS10. The data was fit to a heterogeneous Langmuir model in which the association constant, *K*, is continuously distributed over a finite range of values. The results indicate a small degree of secondary adsorption for all three phases as a separate peak in *K*-space at higher values of *K* than the primary hydrophobic partitioning, and additional adsorption at even higher *K* values for the Zorbax and to a much smaller degree the YMC phase. Integration of the distributions yields the amount of sorption at each of the modeled sites. The results correlate with information known about the synthesis of these phases and the degree of band tailing in elution experiments at these conditions.

Keywords: Sorption isotherms; Stationary phases, LC; Band tailing; Adsorption heterogeneity; Pyridine

1. Introduction

Band tailing in reversed-phase chromatography, especially with basic solutes, has been a long-identified problem. The physicochemical explanation of active sites is also well known. The nature of these active sites is thought to be primarily due to unbonded, residual silanols on the surface of the desilanized silica [1–3]. These silanols become deprotonated at pH values greater than four; thus for basic compounds which are protonated at intermediate pH, strong electrostatic interactions exist that cause the band tailing to higher retention times [4]. It is also recognized that metal impurities can result in surface active sites [5] and the physicochemical nature of the silica and silanols influences the exact nature of the chemical interactions observed with probe solutes [6–8].

Band tailing is often characterized by the amount observed with test solutes [9–11], or alternatively predicted inversely by the silane bonding density or carbon coverage published by manufacturers. The nature of the silanol or active sites has also been published extensively using various techniques

*Corresponding author. Tel.: +1-909-880-7218; fax: +1-909-880-7218.
E-mail address: bstanley@csusb.edu (B.J. Stanley).
[1]Current address: Baxter Healthcare Corporation, 1710 Flower Avenue, Duarte, CA 91010, USA.

0021-9673/03/$ – see front matter
doi:10.1016/S0021-9673(03)01143-9

[2,12–17]. However, an in situ method that provides direct sorptive physicochemical information on the heterogeneous nature of silanol activity beyond the degree of band tailing and bonding can be used that relies on the measurement of sorption isotherms at the chromatographic conditions. Throughout this contribution, a simplification of terms will refer to ''adsorption'' as a ''secondary'' interaction with active sites, ''partitioning'' as the ''primary'' interaction with the bonded-phase, and ''sorption'' will refer to both simultaneously.

Many isotherm measurements, in fact, have *not* been performed under conditions in which band tailing is maximized or is the focus of inquiry. Moreover, most isotherm measurements are performed under a limited concentration range spanning perhaps three to four factors of ten in solute concentration [18–20]. In order to analyze secondary adsorption behavior of the active sites for well-prepared commercial reversed phases, measurements must be taken at very low concentrations because the amount of band tailing is very small and only observable at such concentrations.

In order to characterize the active sites, a heterogeneous sorption isotherm model must be employed. The most common isotherm model employed for reversed phases in preparative applications that utilize the high concentration, partially saturated nonlinear region is the homogeneous Langmuir isotherm [18–20].

One classical model of heterogeneous adsorption is a continuously distributed model of adsorption sites where a representative local model of adsorption is chosen, and this local model is convoluted with a distribution function over a parameter related to the strength or energy of the adsorption [21–23]. This distribution function then characterizes the heterogeneity of the adsorbate–adsorbent interactions and its selective integration yields the maximum amount of adsorption at any given ''site'' or alternatively the site density of the surface. Active sites should result in peak(s) or a finite value for the distribution function at higher binding constants or adsorption energies and the primary partitioning mechanism should be represented by the distribution function at significantly lower sorption energies in accordance with the nature of the band tailing phenomenon. The adsorption distribution approach was developed rather extensively for gas–solid applications, and recently experimental results have been reported for liquid–solid applications [24–29]. For all of the latter liquid–solid applications including molecularly-imprinted polymers (MIPs), chiral, and C_{18} phases, the Langmuir model has been chosen as the local model. This is presumably because of its ubiquitous application and success describing many different types of sorption. It is semi-empirical in nature for this study because the exact mechanism of sorption is unknown with a multicomponent system (pyridine, methanol, water, HCl). The Langmuir model was derived for a binary liquid–solid adsorption system, and thus the rigorous definition of the binding constants in these studies is lacking. As will be shown, a distribution of binding parameters with local Langmuir behavior adequately describes the sorption observed experimentally. The existence of sorption sites with different ''Langmuir-like'' binding parameters reflecting the strength of the interactions is assumed.

The solution of the integral equation that describes the global, experimentally observed, isotherm as a continuous distribution of binding parameters, itself can proceed in a number of directions such as fitting the global isotherm to an empirical or semi-empirical function, and deriving the analytical solution of the distribution function based on the global isotherm parameters [25,26,30–33]. An alternative approach is to use numerical procedures to invert the integral equation to obtain the distribution function without modeling the experimental isotherm beforehand. This latter method amounts to a numerical deconvolution procedure—the deconvolution of adsorption (or partitioning, i.e. sorption) of different energies or binding parameters from the global isotherm according to the local isotherm model. The results of the expectation-maximization (EM) method of numerical estimation have been published for the applications mentioned above [24,28,29]. A regularized least-squares numerical method has also been published for pK_a distributions of heterogeneous iron oxide materials [34]. The analytical solution of a fitted isotherm approach has been extensively published for numerous applications [21–23,25,26,30–33].

In this contribution, the EM estimations of sorption constant distributions obtained from isotherm

data of pyridine retention on three commercial stationary phases is provided. This compound is commonly used in test protocols for band tailing, is a partially ionized base at intermediate pH and thus symptomatic of common band tailing problems, and does not have a large retention factor. Six orders of magnitude in solute concentration are measured encompassing the lowest concentrations that can be detected with common equipment—these lowest concentrations are required to observe and model the active sites. Data of this range on different ODS phases with a common mobile phase and solute, and its heterogeneous modeling has not been demonstrated previously. The methodology is general and can be performed on any sorption system. The isotherm data was acquired using the frontal analysis (FA) method of chromatography; in conjunction with the data analysis, this provides in situ estimates directly representative of the magnitude of the observed chromatographic solute-stationary phase interactions.

In the analysis, it is important to remember that highly efficient, commercial stationary phases were tested. These phases were designed to minimize active or secondary adsorption that leads to band tailing. Therefore the amount of adsorption of this nature is expected to be very small. Previous results with MIPs and chiral protein stationary phases, which are significantly more heterogeneous (more adsorption sites at higher adsorption energies), have been published that validate the methodology [28]. Therefore the current study also demonstrates the low detection limits obtainable with the FA/EM method. It suggests the potential utility of the methodology in studying the physicochemical nature of liquid–solid heterogeneous sorption, and is the first set of results using the general methodology that correlates the obtained distribution functions with chromatographic behavior and manufacturer specifications. Discussion of the details of the isotherm data, distribution function, and application of the EM method are offered to help justify and explain the results.

2. Theory

The theory and methodology of the FA/EM method have been published [24,28,29]. The frontal analysis method has been described extensively [19,35]. Simulation studies and gas–solid applications of the EM method have also been published [36–38], as well as a separate application calculating heterogeneous first-order rate constant distributions [39,40]. The EM method is a general data analysis and deconvolution algorithm [41,42]. Therefore only a synopsis of the calculation of sorption distributions and the EM method is given here.

The general heterogeneous adsorption model can be represented as:

$$q(C) = \int f(\ln K)\theta(K, C)\mathrm{d}\ln K \tag{1}$$

where $q(C)$ is the global, experimentally-determined isotherm, C is the equilibrium mobile phase concentration, $f(\ln K)$ is the distribution function, K is the binding parameter (or sorption constant or affinity constant), and $\theta(K, C)$ is the local adsorption model. It is taken as the Langmuir model in this study. The constant K is exponentially related to the adsorption energy.

The integral is discretized and calculated across a logarithmic K-space:

$$q_{\mathrm{cal}}(C_i) = \sum_{j=1}^{M} f(\ln K_j)\theta(K_j, C_i)\Delta(\ln K) \tag{2}$$

where C_i are the experimentally determined mobile phase concentrations, $\ln K_j$ are the the logarithmic K values in the discretized grid spanning the continuous range, $\Delta(\ln K)$ is the constant logarithmic spacing between these values, and M is the total number of grid points in K-space. The calculation is repeated for each data point, C_i.

In other publications of the general approach [22,25,27,33,36], it is shown that the minimum K_1 is inversely proportional to the maximum concentration, $C_{\max}$, for which isotherm data has been obtained. Conversely the maximum K_M is inversely proportional to the lowest (non zero) concentration data, i.e.

$$K'_{\min} = 1/C_{\max} \text{ and } K'_{\max} = 1/C_{\min} \tag{3}$$

However this is just an approximation of the experimentally determinable range of binding constants. Strictly speaking, an isotherm can be calcu-

lated, Eq. (2), with any range of K values spanning $\ln K_{min}$ and $\ln K_{max}$.

The EM algorithm is iterative, and begins with an initial estimate for the distribution function. The most unbiased approach is to start with a constant distribution across the space defined by $\ln K_{min}$ and $\ln K_{max}$. The ''expectation'' step in the EM algorithm is to calculate the isotherm, via Eq. (2), corresponding to the current guess of the adsorption distribution with the chosen K_j values.

If there is no noise or error in the data and the local isotherm model is correct, the global isotherm equals the experimentally determined isotherm in Eq. (1), i.e. $q(C_i) = q_{exp}(C_i)$, and the correct distribution function perfectly models the isotherm in the absence of numerical errors, i.e.

$$\frac{q_{exp}(C_i)}{q_{cal}(C_i)} = 1 \tag{4}$$

The EM algorithm calculates the actual ratio in Eq. (4) for the current guess of the distribution function, at each data point, and convolutes it with the local model at each grid point to obtain a correction for the distribution function:

$$\beta(\ln K_j) = \sum_{i=1}^{N} \frac{q_{exp}(C_i)}{q_{cal}(C_i)} \theta(K_j, C_i)\Delta(\ln K) \tag{5}$$

where N is the number of data points. The calculation is repeated for each point in the distribution. The distribution function (at each point) is then corrected for a new guess:

$$f(\ln K_j)^k = \beta(\ln K_j) f(\ln K_j)^{k-1} \tag{6}$$

where k is the iteration number. Eqs. (5) and (6) represent the ''maximization'' step in the algorithm. The distribution is corrected so that q_{cal} becomes closer to q_{exp} in accordance with the local model behavior and Eq. (4). Iteration continues by recalculating Eq. (2) with the new guess (expectation), and correcting the distribution accordingly with Eqs. (5) and (6) (maximization). Statistically, iteration should continue until the root mean square (rms) error between q_{cal} and q_{exp} is equal to the rms noise (or error) in the data. Practically, of course, this is not known unless the answer and noise distribution is known beforehand, and a judgement of iteration number must be made.

3. Experimental

3.1. Materials

The technical information published by the manufacturers of the three ODS stationary phases studied are presented in Table 1. All phases are octadecylsilanated silica particles possessing a diameter of 10 μm. Bonded phase density values for Vydac 218TPB (Grace-Vydac, Hesperia, CA) and YMC ODS-A (Waters, Milford, MA) were calculated from the information reported. Vydac reported the amount of silane added before reaction. The surface density reported in Table 1 was obtained assuming 100% reaction, thus resulting in a high-end estimate. YMC reported percent carbon after synthesis. The surface density reported in Table 1 was obtained assuming all of the carbon originated from dimethylchlorooctadecylsilane. Due to endcapping with trimethlylsilane and hexamethyldisilazane, this results in a low-end estimate of bonding density. The Zorbax Pro-10/150 (BTR Separations, Wilmington, DE) value was reported by the manufacturer.

Pyridine was obtained from Aldrich, 99.8%, and used as received. Methanol was HPLC grade from Fisher Scientific and water was obtained from a

Table 1
Manufacturer specifications of the stationary phases studied

Phase	Pore size, Å	Surface area, m^2/g	Bonding	Coverage[a]
Zorbax	150	160	Monomeric, endcapped 1X	2.8 μmol/m^2
Vydac	300	95	Polymeric	16.25% silane added (4.4 μmol/m^2)
YMC	120	300	Monomeric, endcapped 2×	17% carbon (2.4 μmol/m^2)

[a] Values in parentheses are calculated from values listed above them. See text for details.

Barnstead Nanopure water polisher (18.1 $M\Omega^{-1}$ cm, 0.45 μm-filtered) to prepare 60:40 methanol:water mobile phases. The eluent and solutions of pyridine were adjusted to pH 5.0 with HCl. One batch of eluent was used to prepare all solutions and served as the mobile phase for one experiment (all measurements on one phase). The pH was adjusted after preparation using a pH electrode and meter for all concentrated pyridine solutions. The eluent and lowest pyridine concentrations were adjusted by calculation (i.e. HCl added to obtain $[H_3O^+]=1\times 10^{-5}$ *M*). This was determined to be more accurate and consistent then adjustment by measurement because of the inherent poor precision of pH measurements at very low ionic strength.

Six solutions of pyridine were prepared differing in concentration by one factor of ten from approximately 10^{-4} g/l to 10^{1} g/l by serial dilution starting with the most concentrated phase. These six solutions were used for six different FA experiments to cover the entire concentration range of the overall experiment. The exact concentrations used differed slightly in each phase experiment.

Uracil was used to estimate the void volume of the column and mobile phase volume from the eluent mixer on the HPLC to the detector.

3.2. Equipment

An HPLC system (Cole-Scientific, Moorpark, CA) consisting of two Shimadzu LC-10AS pumps was used in the master–slave configuration to perform the FA experiment. The mixer volume was 0.5 ml. The UV/VIS detector was a Shimadzu SPD-10AV and the data acquisition was performed with Axxiom Pyramid software. The stationary phases were packed into 10×0.46 cm stainless steel columns in-house. They were connected to the HPLC in an Eldex column heater and maintained at 30 °C throughout the entire experiment.

3.3. Isotherm (frontal analysis) experiments

The six sub-experiments corresponding to the six concentration ranges measured were performed with slightly different parameters as described below. All experiments were performed at 1.0 ml/min at the temperature and mobile phase conditions noted above. Different wavelengths were used to adjust the detector sensitivity. Different step times were used dependent on the retention times of the different concentrations. Before each sub-experiment range or stage, the column was conditioned with 200 ml of mobile phase at 2.0 ml/min. This step is important to thoroughly cleanse the active sites of pyridine from the previous stage. This volume was determined to be the minimum volume required in separate experiments. A pH of 5 was chosen because it yields deprotonated silanols ($pK_a \approx 4$) and partially protonated pyridine molecules ($pK_a = 5.2$), therefore maximizing electrostatic interactions between adsorbate and adsorbent. This increases retention at the lower concentrations and causes band tailing. The 60:40 methanol:water mobile phase was chosen to reduce overall retention (as well as increase solubility) in order minimize solvent and time costs. At higher water concentrations, especially long run times were incurred at the lowest concentrations for the Zorbax phase. Experiments were run in order from low concentration to high; after the highest concentration range and before the next full experiment, substantial amounts of rinsing of the HPLC system were required to condition it back to the ultra-low concentration levels required at the beginning of a complete experiment.

The experiments were performed by programming the pumps to switch reservoir composition in 10% increments at specified times.

3.3.1. 10^{-5} to 10^{-4} g/l

This lowest-concentration stage yielded the largest retention or breakthrough times. This stage was done manually in FA staircase mode, allowing ample time for breakthrough and equilibration to a new baseline at the new concentration by visual inspection before beginning the next step. The breakthrough time was recorded for a 10% step starting from zero concentration or the pure eluent reservoir. Conditioning as described above is imperative before the first concentration step. Conditioning was not required for subsequent steps, since the next 10% step was performed on top of the previous step. Retention times decreased with step concentration indicating convex-upwards (Langmuir) behavior. The most sensitive wavelength for pyridine (256 nm) was used for this range.

3.3.2. 10^{-4} to 10^{-3} g/l

This stage was done in ''automatic'' staircase mode with 10 min steps programmed on the master pump starting from zero concentration. The retention times decreased with concentration and approached a constant value after a few steps in this stage. The detection wavelength was 256 nm.

3.3.3. 10^{-3} to 10^{-2} g/l

The step time was decreased to 5 min. The retention time quickly approached a constant value in this stage and remained this value for the remaining stages performed, and thus 5 min was used for the remaining stages' step time. The detector wavelength was 256 nm.

3.3.4. 10^{-2} to 10^{-1} g/l

The wavelength was increased to 262 nm, because of detector saturation at 256 nm.

3.3.5. 10^{-1} to 10^{0} g/l

The wavelength was increased to 270 nm.

3.3.6. 10^{0} to 10^{1}g/l

The wavelength was increased to 275 nm.

The detection of mobile phase concentration was determined for each wavelength and range using least-squares analysis of the plateau detector signal vs. the known concentration at the plateau. A cubic polynomial was required for the highest two concentration ranges obtained at 270 and 275 nm. The isotherm was then calculated with the frontal analysis equations [35]:

$$q_{i+1} = q_i + \frac{(C_{i+1} - C_i)(V_{F,i+1} - V_0)}{V_a} \quad (7)$$

where V_F is the retention volume, V_0 is the total void volume, and V_a is the adsorbent volume. The ranges were then connected together to form the entire-range isotherm spanning six orders of magnitude in pyridine concentration. The Zorbax concentration range was 5×10^{-5} to 5×10^{1} g/l. This corresponds to an ''effective'' K'-range of 2×10^{-2} to 2×10^{4} l/g via Eq. (3); the corresponding values for YMC were 1×10^{-5} to 1×10^{1} g/l with $K'=1\times10^{-1}$ to 1×10^{5} l/g and for Vydac $C=2\times10^{-5}$ to 2×10^{1} g/l with $K'=5\times10^{-2}$ to 5×10^{4} l/g.

The column void volume was obtained by subtracting the volume obtained with the column replaced by a low-volume union from the total void (mobile phase) volume. The stationary phase volume was then obtained by subtracting the column void volume from the geometric (empty) column volume. These volumes along with the adsorbent masses, total surface areas and octadecylsilane are given in Table 2.

4. Computational

The EM algorithm was programmed in Fortran (Lahey/Fujitsu Fortran 95, Incline Village, NV). One hundred points in K-space were chosen to digitize the range logarithmically between $K_{min}=2\times10^{-4}$ l/g and $K_{max}=2\times10^{4}$ l/g. A K_{min} value one hundred times less than K'_{min} (from Eq. (3)) was chosen because the calculated distributions were divergent at K'_{min}. The large majority of the sorption was due to partitioning and the central K value for this partitioning is possibly less than K'_{min}. This is a common problem and result of this type of data analysis of sorption isotherms [27,28,37,38], and is discussed further along with the results in the next section. Decreasing K_{min} beyond K'_{min} in the distribution calculation deconvolutes low-K information (low energy partitioning) away from the higher energy-K

Table 2
Column stationary phase parameters

Phase	Volume (ml)	Mass[a] (g)	Total surface area (m^2)	Amount of C_{18} silane (μmol)
Zorbax	0.75	1.2	190	540
Vydac	0.55	0.9	85	370
YMC	0.55	0.9	260	630

[a] Assumes silica density is equal for three phases.

information. The result is a better fit to the data at high concentrations while still fitting the low concentration data well with higher K constants. In summary, K_{min} and K_{max} were used to calculate the distribution with the EM algorithm, but K'_{min} and K'_{max} were used to define the ''effectively-modeled'' region in which the distribution may be interpreted with more confidence. This latter region is that graphed in the results.

Ten thousand iterations were performed by the algorithm. With a Pentium II 350 MHz computer, one hundred K points and 55 data points, this calculation takes less than 10 s. In the presence of experimental error, excessive iteration causes irreproducible, artifactual information in the distribution function uncorrelated with physicochemical phenomena as Eq. (4) is approached. The algorithm has been shown in general to suppress artifactual information (i.e. provide ''smooth'' distributions) compared to other techniques [36,39]. Major peaks required to fit the data according to the Langmuir local model develop early in the iteration sequence; insignificant change exists between 10^3 and 10^5 iterations; artifacts can develop as 10^6 iterations are approached. Resolution increases with iteration and thus is sacrificed to some degree for smoothness with this choice. In general, further iteration can be attempted to increase resolution by accepting the risk of artifacts.

The differential saturation capacity at each point, $q_S(K_j)$:

$$q_S(K_j) = f(\ln K_j)\,\Delta(\ln K) \tag{8}$$

is plotted against $\log_{10} K_j$ as the sorption distributions in the results that follow. The values comprising one peak in the distribution can then be added to obtain the saturation capacity or maximum adsorption at one ''type'' of site possessing a mean K-value.

5. Results and discussion

The experimental isotherms along with the final calculated isotherm fit determined from the sorption distributions are shown in Fig. 1 in log–log form, which illustrates all of the data. At low concentrations, Zorbax sorbs more than the other two phases. At higher concentrations, the differences are less noticeable. The YMC phase has a higher sorption constant than Vydac at low concentrations but slightly lower at higher concentrations. The degree of heterogeneity in these phases is very small due to similar octadecylsilanization and deactivation of silanol sites. It cannot be observed sigmoidally in log–log form because the change in slope is too small and subtle. It can be observed, however, by careful inspection of the isotherms in normal view without logarithms. The lowest concentration data is plotted in Fig. 2. The slope is seen to be greater as the concentration decreases, and this effect is the most notable for the Zorbax phase. In fact, if the

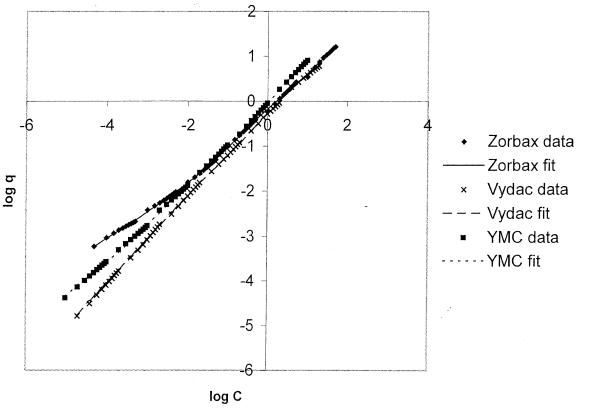

Fig. 1. Full-range isotherm data for phases studied along with fits corresponding to Langmuir distribution model.

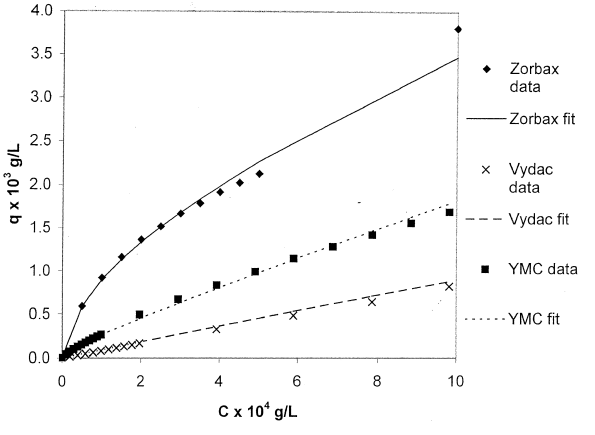

Fig. 2. Lowest concentration range of isotherm data along with fits corresponding to Langmuir distribution model.

instantaneous slope is followed through the higher concentrations, it is seen to decrease with concentration in all cases; the decreasing change becomes less with increasing concentration. At the highest concentrations, the isotherms are fairly linear.

This behavior displays heterogeneity. If homogeneous partitioning were operative throughout the concentration range, the isotherms would be linear from the origin. The degree of nonlinearity occurs to the greatest extent at the lowest concentrations, but does not extend far, which suggests that a small amount of higher energy adsorption exists. The linearity at higher concentration is because the partitioning sorption is not saturated. In fact, this high capacity linearity reduces the nonlinearity of the low concentration region. The data suggests that the saturation capacity of the low energy partitioning mechanism is much greater than the higher energy adsorption attributable to active sites (slope = distribution constant $= K_D = \Sigma_j\ q_{S,j}K_j$ in discretized distribution model). However, it is clear from the data that higher energy adsorption, with correspondingly higher K values is occurring. Deconvolution of this higher energy adsorption data would indicate the magnitude of K and its saturation capacity according to Eqs. (1) and (7). Since the general linearity decreases in the order Vydac > YMC > Zorbax, the heterogeneity should increase in this order. However, the nature of the heterogeneity (q_S vs. K) is not obtainable with these types of observations.

In representative previously published isotherm data of C_{18} phases, the mobile phase concentration ranges from approximately 10^{-2} or 10^{-3} to over 10^{1} g/l [18–20,29]. No special notes of mobile phase conditions conducive to band tailing were made. In this study, conditions were set at those in which band tailing was observed, and the isotherms were measured down to 10^{-5} g/l. Extensive conditioning at pH 5 was performed prior to each run. Therefore, it is important to note that the experiment was conducted specifically to detect active site retention in the isotherm data. For well-manufactured commercial phases in which this behavior is minimized, it cannot be detected in higher concentration isotherm data as previously performed in other studies [29].

The heterogeneity is modeled in the distributions calculated from the global isotherms; these are given in Figs. 3–5. Pertinent results obtained from the distributions are summarized in Table 3.

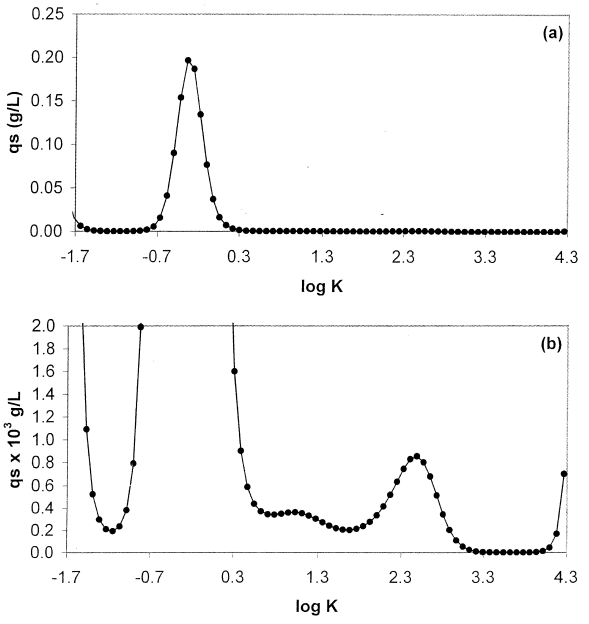

Fig. 3. (a) Sorption distribution model for Zorbax stationary phase illustrating majority of active sites. Partitioning sorption occurs at log $K < -1.7$. (b) Magnification of sorption distribution illustrating small amount of adsorption with higher binding constants.

The distributions diverge off-scale in the illustrations around $K'_{\min}$ due to the undersampled hydrophobic partitioning mechanism for which the stationary phases are designed. This is considered K_1 in the model results. The small degree of heterogeneity and

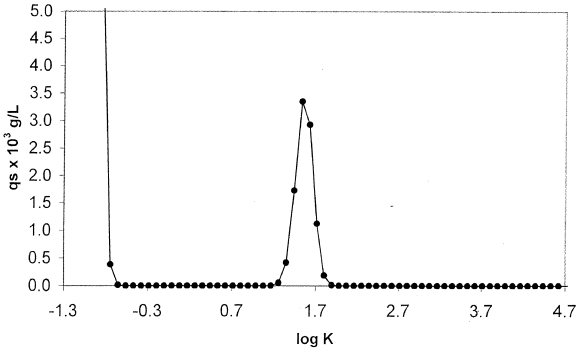

Fig. 4. Sorption distribution model for Vydac stationary phases illustrating majority of active sites. Partitioning sorption occurs at log $K < -1.0$.

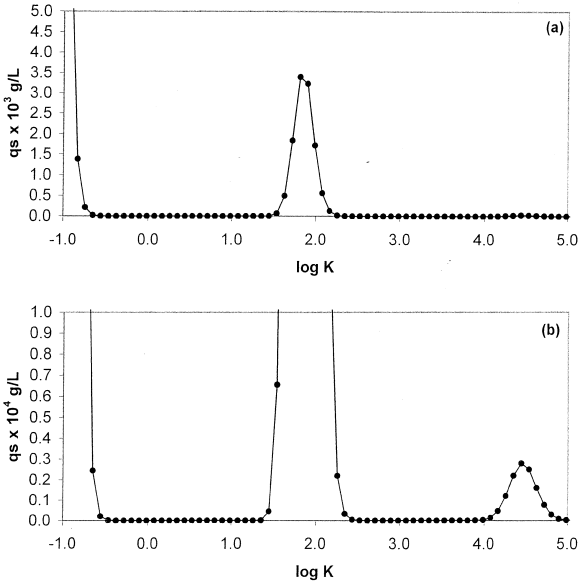

Fig. 5. (a) Sorption distribution model for YMC stationary phases illustrating majority of active sites. Partitioning sorption occurs at log $K<-0.8$. (b) Magnification of sorption distribution illustrating a very small amount of adsorption with a high binding constant.

active sites observed for these phases is displayed as peaks throughout the remainder of the K-range. The higher slope isotherm data at the lower concentrations cannot be fit (see Fig. 2) without the information at these higher K values. The K_1 information obtained is in agreement with the order of magnitude published for C_{18} phases and similar systems with the Langmuir model ($K_1 \approx 10^{-2}$ L/g and $q_{S,1} \approx 10^2$ g/l) [18–20,29]. It is determined here between the specified K_{min} in the algorithm and K'_{min} defined by Eq. (3), i.e. $K_{min} < K_1 < K'_{min}$. The active sites are observed at $K > 0.1$ l/g $> K'_{min}$.

Although the high concentration data is fit well with the model, a narrow peak representative of relatively homogeneous partitioning is not obtained since not enough curvature at the high concentration end of the isotherm was obtained. Without prior knowledge in an unbiased model, possible lower-K sorption or further sorption at higher concentration may occur. In previous isotherm studies, concave-upwards behavior was noted at high solute concentrations for C_{18} phases for some solutes [20,24]. In almost all isotherm studies, the experimental maximum concentration is limited by solubility considerations [28,29]. In other isotherm studies with different models such as the Freundlich isotherm, the theoretically expected distribution function is itself divergent at K'_{min} [21,26,27]. These results and considerations suggest that the lowest sorption energies may be intractable as a narrow peak in the distribution function. However, results have been published with the EM method suggesting that the calculated information at higher adsorption energies is not affected substantially by this phenomena, i.e. it is successively deconvoluted [36–38]. In the results of this study, it can therefore be concluded that the lower energy partitioning, corresponding to the linearity of the isotherm, is successfully separated from the active adsorption. However, $q_{S,1}$ and K_1 cannot be reported with confidence because of the lack of sampling at very high concentration.

Both similarities and differences in the heterogeneity of these phases are observed. Zorbax has a considerably large peak at $K = 0.45$. All three phases exhibit adsorption in the range log $K = 1$–2. The Zorbax and YMC phases exhibit further heterogeneity at higher K-values. The Zorbax model shows two unresolved peaks on the tail of K_2, and a divergence at $K'_{max} = 18{,}300$ (these are all grouped as K_3 in Table 3). This latter divergence occurs because additional data at concentrations less than 5×10^{-5} g/l is required to sample it. The YMC phase displays a very small adsorption peak at very high $K = 28{,}000$. In the YMC experiment we were able to obtain data points down to 1×10^{-5} g/l. In the

Table 3
Summary of sorption distributions obtained for pyridine on stationary phases in 60:40 MeOH:H_2O at pH 5

Phase	$K_{2,mean}$ (l/g)	$q_{S,2}$ (g/l)	$K_{3,mean}$ (l/g)	$q_{S,3}$ (g/l)
Vydac	34	0.0098	–	–
YMC	64	0.011	28,000	0.00012
Zorbax	0.45	0.97	11, 305, >18,000	0.0032, 0.0078, 0.00093

Zorbax experiment, retention was too long at $C < 5 \times 10^{-5}$ g/l, resulting in very diffuse breakthroughs that were not sufficiently reproducible.

The model results suggest that a similar type of active site, characterized by log $K \approx 1$–2, causes nonlinearity in the low concentration region of all three phase isotherms. At very low concentrations, the Zorbax model requires additional active sites with higher K values to describe the data. The Zorbax model requires a very small amount of adsorption at high K to help fit the first couple of isotherm data points which resulted from significantly greater breakthrough retention times than that observed in the remainder of the experiment (see Fig. 2). The magnitude of the q_S values observed for the active sites in the phases correspond to the increased adsorption observed in the isotherms at the lower concentrations shown in Fig. 2. The results show increasing heterogeneity in the order Vydac < YMC < Zorbax both in terms of q_S and K.

The results are in agreement with the degree of band tailing observed for pyridine in elution experiments illustrated in Fig. 6. Band tailing increases with heterogeneity and the detection of active sites. The tailing continues at very low concentrations for YMC (barely noticeable in Fig. 6) but does not with Vydac, due to the very small, high energy adsorption site detected for YMC (but not for Vydac). The Zorbax phase tails at intermediate, low and very low concentrations due to the much greater heterogeneity observed for this phase throughout the K-range. This band tailing is explained with the notion of active sites. Information corresponding to these active sites is imprinted in the isotherm data and revealed upon deconvolution in the sorption distribution. Furthermore, as shown in a previous publication, band tailing of this nature cannot be modeled without a heterogeneous distribution of sorption constants if the equilibrium-dispersive model is used [24].

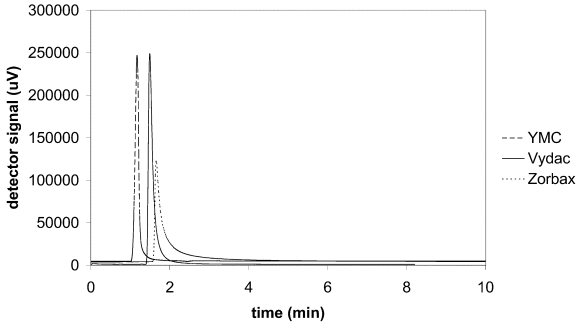

Fig. 6. Chromatograms of pyridine elution (1.0 g/l, 10 μl injection) at conditions under which isotherms were measured (60:40 MeOH:H_2O, pH 5, 30 °C, 1.0 ml/min, 10×0.46 cm column) for stationary phases studied.

These results are also correlated with the known bonding of the stationary phases. The Vydac polymerized phase has the largest amount of silane attached to the silica surface per area, and therefore presumedly the lowest accessibility to unbonded active sites. Coupled with the lowest surface area of the three, this is in agreement with the lowest detected saturation capacity of the active sites. The higher hydrocarbon density of Vydac, possibly coupled with the greater pore size, results in the greater retention with respect to YMC at higher concentrations. The YMC has the lowest bonded-phase coverage, but it is end-capped twice, and this should result in lower accessibility to active sites by the pyridine molecules in this study relative to Zorbax. The high surface area of YMC probably allowed the detection of some these sites at low concentrations. Possibly similar high energy sites might not have been detected for Vydac due to its low surface area.

The silanol surface density of typical silicas is often reported as 7–8 μmol/m^2 [7]. Using the higher end of this estimate, the bonded phase coverage is only 30% (YMC, low estimate), 35% (Zorbax, manufacturer's estimate) and 55% (Vydac, high estimate assuming 1:1 silane:silanol attachment). It should be noted that this experiment probes sites activated under the conditions of the study and does not necessarily have to follow a trend in bonded phase coverage. The physicochemical nature of the base silica and its silanol sites (e.g. ''free'' vs. hydrogen-bonded) is also very important in defining types and amounts of active sites in addition to the bonding chemistry [2,12,13]. Indeed, the results suggest that this is the case for the Zorbax phase since it is significantly more heterogeneous than either of the other two phases. Although the results in general seem to verify the well-known and followed maxim of decreasing silanol activity by increasing bonded-phase coverage either with polymerization or with additional end capping, they also suggest the physicochemical basis of band tailing for

Zorbax has other factors at play. This demonstrates the utility of the methodology in characterizing the nature of the chromatographically observed surface heterogeneity.

In recent work utilizing the FA/EM method for the study of enantiomer-selective adsorbent heterogeneity, higher energy adsorption was observed for only the selective enantiomer; the distribution function was drastically reduced or nonexistent at higher energies for the nonselective enantiomer [28]. These observations held even though the low energy nonselective sorption was also undersampled in those studies. Considering this and other previous experimental work [24], previous simulations of this nature [37–39], and the experimental correlations with separate measurements reported here, the small amplitude of information at high energy is considered beyond artifactual. It is indicative of real phenomena. Unfortunately, the accuracy and precision of the methodology is poorly defined because a standard reference material of known heterogeneity is not available, solution of Eq. (1) is ill-defined (many solutions possible with same data if error is present), and the exact nature of a bonded surface itself may not be reproducible from experiment-to-experiment. Therefore the method should only be considered a tool in the characterization of heterogeneous sorption. Its ability to precisely and accurately determine physicochemical sorption parameters requires further definition and/or development. Research of this nature is currently underway.

6. Conclusions

The FA/EM method of calculating sorption distributions for analysis of heterogeneity can be applied to commercial reversed-phase stationary phases. A very large range of concentration data must be obtained because a very small amount of the higher energy secondary adsorption occurs with these phases in the presence of the designed low energy partitioning. Mobile phase conditions conducive to band tailing must be applied. The active sites can be detected in the sorption distributions as separate peaks at higher energy. Similarities in the high energy adsorption exist for different commercial phases, suggesting similar types of unreacted silanol sites; however, differences also exist that suggest further specific type(s) of adsorption interactions. The results are in correlation with the manufacturer's bonding specifications and the nature of band tailing observed in separate experiments. However, such analysis and characterization is not possible with simple observation of the adsorption isotherms, chromatograms, or bonding density alone. In combination with other methods for characterizing microheterogeneity or silanol activity [2,12–17], the methodology can facilitate thermodynamic information into a more comprehensive characterization of the in situ adsorption heterogeneity observed of analytical or other types of sorbents.

Acknowledgements

This research was supported by the donors of The Petroleum Research Fund administered by the American Chemical Society.

References

[1] L.R. Snyder, J.J. Kirkland, Introduction to Modern Liquid Chromatography, 2nd ed., Wiley, New York, 1979.
[2] J. Köhler, J.D.B. Chase, R.D. Farlee, A.J. Vega, J.J. Kirkland, J. Chromatogr. 352 (1986) 275.
[3] E. Meyer, H. Engelhardt, Fesenius' Z. Anal. Chem. 333 (1989) 734.
[4] R.W.P. Fairbank, M.J. Wirth, Anal. Chem. 69 (1997) 2258.
[5] K. Kimata, N. Tanaka, T. Araki, J. Chromatogr. 594 (1992) 87.
[6] J. Köhler, J.J. Kirkland, J. Chromatogr. 385 (1987) 125.
[7] K.K. Unger, Porous Silica, Elsevier, Amsterdam, 1979.
[8] R.K. Iler, The Chemistry of Silica, Wiley, New York, 1979.
[9] H. Engelhardt, H. Löw, W. Götzinger, J. Chromatogr. 544 (1991) 371.
[10] D.V. McCalley, J. Chromatogr. A 738 (1996) 169.
[11] D.V. McCalley, J. Chromatogr. A 769 (1997) 169.
[12] C.H. Lochmüller, D.B. Marshall, D.R. Wilder, Anal. Chim. Acta 130 (1981) 31.
[13] C.H. Lochmüller, A.S. Colborn, M.L. Hunnicutt, J.M. Harris, Anal. Chem. 55 (1983) 1344.
[14] C.H. Lochmüller, A.S. Colborn, M.L. Hunnicutt, J.M. Harris, J. Am. Chem. 106 (1984) 4077.
[15] J.W. Carr, J.M. Harris, Anal. Chem. 58 (1986) 626.
[16] S.C. Rutan, J.M. Harris, J. Chromatogr. A 656 (1993) 197.
[17] L.A. Ciolino, J.G. Dorsey, J. Chromatogr. A 678 (1994) 201.
[18] J. Jacobson, J. Frenz, Cs. Horváth, J. Chromatogr. 316 (1984) 53.

[19] J.-X. Huang, Cs. Horváth, J. Chromatogr. 406 (1987) 275.
[20] H. Guan, G. Guiochon, J. Chromatogr. A 687 (1994) 179.
[21] A.W. Adamson, Physical Chemistry of Surfaces, John Wiley & Sons, New York, 1982, Chapters 11 and 16.
[22] M. Jaroniec, R. Madey, Physical Adsorption on Heterogeneous Solids, Elsevier, Amsterdam, 1988.
[23] W. Rudzinski, D.H. Everett, Adsorption of Gases on Heterogeneous Surfaces, Academic Press, New York, 1992.
[24] B.J. Stanley, J. Krance, A. Roy, J. Chromatogr. A 865 (1999) 97.
[25] R.J. Umpleby II, M. Bode, K. Shimizu, Analyst 125 (2000) 1261.
[26] R.J. Umpleby II, S.C. Baxter, Y. Chen, R.N. Shah, K.D. Shimizu, Anal. Chem 73 (2001) 4584.
[27] P. Szabelski, K. Kaczmarski, A. Cavazzini, Y.-B. Chen, B. Sellergren, G. Guiochon, J. Chromatogr. A 964 (2002) 99.
[28] B.J. Stanley, P. Szabelski, Y.-B. Chen, B. Sellergren, G. Guiochon, Langmuir 19 (2003) 772.
[29] G. Gritti, G. Götmar, B.J. Stanley, G. Guiochon, J. Chromatogr. A 988 (2003) 185.
[30] D.L. Hunston, Anal. Biochem. 63 (1975) 99.
[31] A.K. Thakur, P.J. Munson, D.L. Hunston, D. Rodbard, Anal. Biochem. 103 (1980) 240.
[32] W. Rudzinski, J. Jagiello, Y. Grillet, J. Coll. Int. Sci. 87 (1982) 478.
[33] J. Jagiello, G. Ligner, E. Papirer, J. Coll. Int. Sci. 137 (1990) 128.
[34] D.S. Smith, F.G. Ferris, Environ. Sci. Technol. 35 (2001) 4637.
[35] G. Guiochon, S. Golshan-Shirazi, A.M. Katti, Fundamentals of Preparative and Nonlinear Chromatography, Academic Press, New York, 1994, Chapter 3.
[36] B.J. Stanley, G. Guiochon, J. Phys. Chem. 97 (1993) 8098.
[37] B.J. Stanley, G. Guiochon, Langmuir 10 (1994) 4278.
[38] B.J. Stanley, G. Guiochon, Langmuir 11 (1995) 1735.
[39] B.J. Stanley, S.E. Bialkowski, D.B. Marshall, Anal. Chem. 65 (1993) 259.
[40] B.J. Stanley, K. Topper, D.B. Marshall, Anal. Chim. Acta 287 (1994) 25.
[41] W.H. Richardson, Opt. Soc. Am. 62 (1972) 55.
[42] S.E. Bialkowski, J. Chemom. 52 (1991) 11.